AMERICAN SOCIETY FOR MICROBIOLOGY | Infection and Immunity®

CELLULAR MICROBIOLOGY:
PATHOGEN-HOST CELL MOLECULAR INTERACTIONS

The Extracellular Polysaccharide Matrix of *Pseudomonas aeruginosa* Biofilms Is a Determinant of Polymorphonuclear Leukocyte Responses

Morten Rybtke,[a] Peter Østrup Jensen,[a,b,c] Claus Henrik Nielsen,[c] Tim Tolker-Nielsen[a]

[a]Costerton Biofilm Center, Department of Immunology and Microbiology, University of Copenhagen, Copenhagen, Denmark
[b]Department of Clinical Microbiology, Copenhagen University Hospital (Rigshospitalet), Copenhagen, Denmark
[c]Center for Rheumatology and Spine Diseases, Institute for Inflammation Research, Copenhagen University Hospital (Rigshospitalet), Copenhagen, Denmark

ABSTRACT Bacterial biofilms may cause chronic infections due to their ability to evade clearance by the immune system and antibiotics. The persistent biofilms induce a hyperinflammatory state that damages the surrounding host tissue. Knowledge about the components of biofilms that are responsible for provoking the harmful but inefficient immune response is limited. Flagella are known to stimulate the response of polymorphonuclear leukocytes (PMNs) to planktonic solitary bacteria. However, we provide evidence that flagella are not a prerequisite for the response of PMNs to *Pseudomonas aeruginosa* biofilms. Instead, we found that extracellular matrix polysaccharides in *P. aeruginosa* biofilms play a role in the response of PMNs toward biofilms. Using a set of *P. aeruginosa* mutants with the ability to produce a subset of matrix exopolysaccharides, we found that *P. aeruginosa* biofilms with distinct exopolysaccharide matrix components elicit distinct PMN responses. In particular, the PMNs respond aggressively toward a biofilm matrix consisting of both Psl and alginate exopolysaccharides. These findings are relevant for therapeutic strategies aimed at dampening the collateral damage associated with biofilm-based infections.

KEYWORDS biofilm, PMN, alginate, Psl, *Pseudomonas aeruginosa*, biofilms, polymorphonuclear leukocytes

It is well established that most chronic bacterial infections involve biofilms, which are heaps of bacteria encased in an exopolymeric matrix composed of polysaccharides, DNA, proteins, and lipids. The biofilms may be adherent to a living or inert surface, e.g., the cornea, prosthetic joints, or other implants (1). They may also exist as aggregates suspended in the extracellular milieu, e.g., in the thickened mucus found in the lungs of cystic fibrosis (CF) patients or in chronic wounds (1, 2).

Common to the biofilm variants is their ability to withstand attack by the host immune system, of which innate immune cells, particularly the polymorphonuclear leukocytes (PMNs), are key players. As a first line of defense, PMNs are summoned to the site of infection, where they generate and release reactive oxygen species (ROS) during the oxidative burst and instigate degranulation, phagocytosis, and expulsion of neutrophil extracellular traps (NETs) in an attempt to combat the microbes and resolve the infection (3, 4). Despite the alertness of the immune system, the biofilm mode of life enables the bacteria to evade the immune response and persist. This standoff between immune cells and biofilm eventually leads to a chronic inflammation, which results in collateral damage of the surrounding host tissue (5). Although tissue destruction mediated by PMNs is a common denominator of various biofilm-based infections, there is a lack of knowledge about which components of biofilms

Citation Rybtke M, Jensen PØ, Nielsen CH, Tolker-Nielsen T. 2021. The extracellular polysaccharide matrix of *Pseudomonas aeruginosa* biofilms is a determinant of polymorphonuclear leukocyte responses. Infect Immun 89:e00631-20. https://doi.org/10.1128/IAI.00631-20.

Editor Manuela Raffatellu, University of California San Diego School of Medicine

Address correspondence to Tim Tolker-Nielsen, ttn@sund.ku.dk.

Received 8 October 2020
Accepted 9 October 2020
Accepted manuscript posted online 19 October 2020
Published 15 December 2020

are responsible for activation of the innate immune system. Consequently, there is a need to understand the interaction between immune cells and biofilms, as well as the properties of the biofilms that lead to inflammation without efficient resolution. Such knowledge may form a basis for development of new and effective treatment strategies.

The opportunistic pathogen *Pseudomonas aeruginosa* is a common cause of chronic infections and is the archetypal biofilm-forming pathogen in cystic fibrosis lung infections and chronic wounds (6). *P. aeruginosa* can synthesize three different matrix exopolysaccharides, Pel, Psl, and alginate (7–9), but the ability to do so varies between strains and clinical isolates (10, 11). The common laboratory strain *P. aeruginosa* PAO1 produces both Pel and Psl under standard conditions, whereas stringent transcriptional repression of the operon encoding the synthesis machinery prevents it from producing alginate (12). Alginate production is mostly observed for clinical *P. aeruginosa* isolates of the mucoid morphotype and typically originates from derepressing genetic adaptations (13, 14). Overproduction of Pel and Psl, resulting in hyper-biofilm formation, is observed for clinical isolates of *P. aeruginosa* rugose small colony variants (RSCVs) that display an increased level of the second messenger cyclic di-GMP, which is a positive regulator of the biosynthesis of various biofilm matrix components (15–17). Alginate is known to protect biofilm bacteria by reducing phagocytosis by macrophages and PMNs (18, 19) and by scavenging damaging ROS (20, 21). Psl has been shown to protect biofilm bacteria from opsonization-mediated PMN and macrophage responses by decreasing complement deposition on the bacteria (22). No specific biofilm-protecting role of Pel has been described to date, but an *in vitro* study of exopolysaccharide-overproducing RSCVs with a deficiency in Pel synthesis suggests that Pel is involved in protecting the bacteria from phagocytosis by macrophages (16).

Planktonic single cells of *P. aeruginosa* are known to be recognized by the innate immune system through pathogen-associated molecular patterns (PAMPs), such as the flagellum and lipopolysaccharide (LPS), which are recognized via Toll-like receptors 5 and 4, respectively (23, 24). Recent evidence also suggests that motion of the flagellum, and not the flagellum *per se*, plays a role in the immunogenicity through a Toll-like receptor-independent mechanism (25). When residing in a biofilm, however, the bacteria are embedded in extracellular polymeric substances, and the classical PAMPs are most likely less exposed to the immune system. There is evidence to suggest that the adaptive immune system responds to components of the *P. aeruginosa* biofilm matrix. Thus, antibodies against the alginate polysaccharide can be isolated from CF patients infected with mucoid *P. aeruginosa*, although they fail to aid in the clearance of the infection (26). In the case of the innate immune system, the available evidence suggests that aggregation of biofilm bacteria is important for eliciting a strong immune response. Thus, *P. aeruginosa wspF* RSCVs formed aggregates and stimulated a stronger PMN response than the isogenic wild type, which did not form aggregates (27). Exposure of PMNs to purified Pel and Psl polysaccharide did not elicit a strong PMN response, whereas the PMNs responded vigorously to aggregates of a *P. aeruginosa* strain deficient in Pel and Psl production (27). In the latter case, aggregation of the bacteria was achieved by overexpression of the adhesin CdrA, but purified CdrA did not elicit a PMN response (27). The ability of purified cell-free biofilm matrix polysaccharides to activate innate immune cells has also been investigated by others, and their results suggest that the response is strain dependent but low (28, 29).

Despite the low immunostimulatory ability of purified biofilm matrix polysaccharides, and the apparent ability of matrix-independent bacterial aggregates to induce a strong innate immune response, it is possible that specific bacterial components of the biofilms may play distinct roles in activating the immune cells. In the current study, we investigated the involvement of flagella and exopolysaccharide matrix components in the induction of PMN responses to *P. aeruginosa* biofilms. We hypothesized that flagella are not important for the PMN response to biofilms, because of embedment of the bacteria in the extracellular matrix and a concomitant impediment of the bacterial

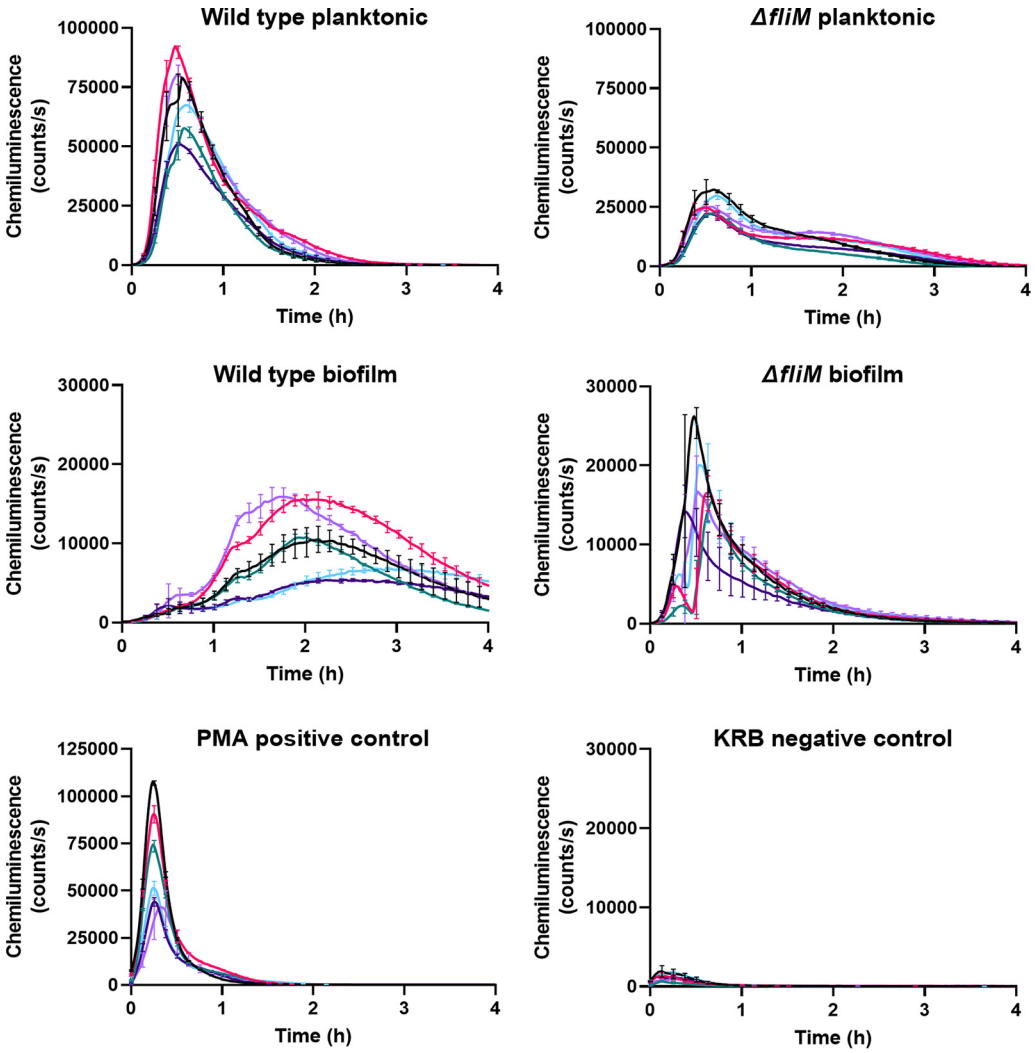

FIG 1 Oxidative-burst response of polymorphonuclear leukocytes (PMNs) toward the *P. aeruginosa* PAO1 wild type and an isogenic nonflagellated *fliM* mutant growing as planktonic bacteria or biofilms. The planktonic samples consisted of exponentially growing bacteria challenged with PMNs at time zero. The biofilms were grown in microplate wells and were subsequently washed carefully to remove planktonic cells, before PMNs were added at time zero. Luminol-enhanced chemiluminescence was used as a measure of the oxidative burst of PMNs. Phorbol 12-myristate 13-acetate (PMA) was used as a positive control of reactive oxygen species release by the PMNs. Krebs-Ringer buffer supplemented with 10 mM glucose (KRB) was used as a negative control. PMNs were purified from the blood of healthy human volunteers. Complete chemiluminescence curves from six donors are shown as averages of three technical replicates. Individual *y* axis scales were used for proper comparison of the different conditions. Error bars indicate standard deviations.

appendages. Moreover, we hypothesized that specific components of the extracellular matrix determine the strength of the PMN response to the biofilms, since these components are exposed to the immune cells. The hypotheses were tested by monitoring the response of isolated human PMNs to planktonic bacteria and biofilms of *P. aeruginosa*, using a set of mutants with flagellum deficiency or the ability to produce a defined subset of matrix exopolysaccharides.

RESULTS

Flagella do not play an important role for the response of PMNs to *P. aeruginosa* biofilms. We assessed the oxidative-burst response of PMNs from six healthy donors toward planktonic wild-type *P. aeruginosa* PAO1 and an isogenic nonflagellated mutant (*fliM*), using a luminol-enhanced chemiluminescence assay. Figure 1 shows the PMN oxidative-burst response as a function of time. Exposure of PMNs to the planktonic bacteria markedly increased the chemiluminescence signal, indicating that the PMNs

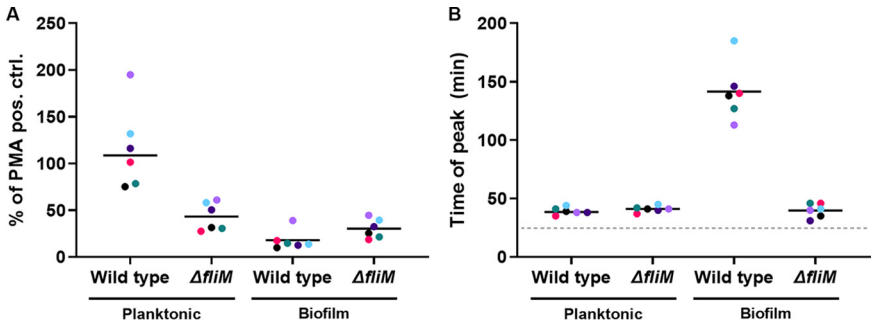

FIG 2 Parameters characterizing the oxidative-burst response of PMNs toward the *P. aeruginosa* PAO1 wild type and an isogenic nonflagellated *fliM* mutant. The parameters are derived from the chemiluminescence curves shown in Fig. 1. (A) Peak chemiluminescence levels normalized to those of cells incubated with the positive control PMA. (B) Time point of the peak chemiluminescence level. The punctured gray line shows the average peak time of the PMA-stimulated positive controls. Symbol color indicates the individual donors ($n = 6$). Data points shown for each donor are the averages of three technical replicates. The horizontal bar indicates the mean across all donors.

became activated (Fig. 1, compare upper graphs to the lower right graph). Moreover, it is evident that the flagellated planktonic bacteria elicited a stronger PMN response than the nonflagellated planktonic bacteria (Fig. 1, upper graphs).

Two variables were used to describe the PMN response: peak levels of chemiluminescence, corresponding to the strength of the response, and time of peak occurrence after challenge, corresponding to the swiftness of the response. The data shown in Fig. 2A are normalized to the phorbol 12-myristate 13-acetate (PMA) positive control (Fig. 1, lower left graph) to compensate for the biological variation between PMNs from the different donors. The PMN response against planktonic bacteria was significantly less potent when flagella were absent (Fig. 2A) ($P = 0.01$; see Table S1 in the supplemental material for complete comparative statistics), with a minor, yet significant, difference in timing of the response (Fig. 2B and Table S1).

Having thus demonstrated the importance of flagella in induction of PMN responses to planktonic *P. aeruginosa* bacteria, we subsequently investigated the involvement of flagella in the response of PMNs toward *P. aeruginosa* growing as a biofilm. To this end, a biofilm assay was developed using optical-bottom microplates. The optical bottom enabled imaging of the biofilm structures using confocal laser scanning microscopy, providing an opportunity to relate the biofilm structure to the response of the PMNs. As shown in Fig. 3 and Table 1, the *P. aeruginosa* wild type and the *fliM* mutant developed biofilms of similar natures and sizes, with the biofilm of the wild type being slightly more structured and with a more heterogeneous surface colonization. The structural difference may result from the known involvement of flagellum-based swimming motility in microcolony development (30, 31). The biomass quantification was

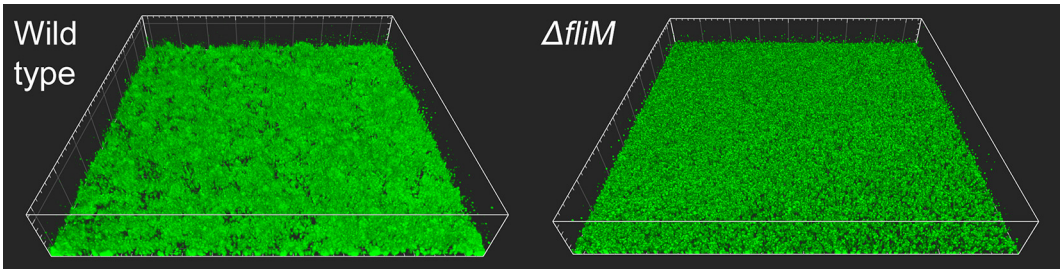

FIG 3 Biofilms formed by the *P. aeruginosa* PAO1 wild type and a *fliM* mutant at the bottom of microplate wells. Biofilms were established under static conditions for 24 h at 37°C, subsequently washed to remove planktonic cells, and stained with the green fluorescent dye Syto9 for visualization. Images displayed are three-dimensional (3D) projections of image stacks captured using confocal laser scanning microscopy and a 20×/0.8 air objective. Grid size is 50 μm.

TABLE 1 Biofilm biomass quantification[a]

Strain description	Biofilm biomass, $\mu m^3/\mu m^2$	% of type
Wild type	7.85 (0.39)	100
Δ*fliM*	6.10 (0.30)	78
Pel^+ (Psl^- Alg^-)	6.20 (0.52)	79
Psl^+ (Pel^- Alg^-)	6.47 (0.19)	82
Alg^+ (Pel^- Psl^-)	3.05 (0.14)	39
Alg^+ Pel^+ (Psl^-)	4.77 (0.26)	61
Alg^+ Psl^+ (Pel^-)	5.63 (0.24)	72

[a]Biomass was quantified from confocal laser scanning microscope image stacks using Imaris image analysis software. Data are presented as averages (SDs in parentheses) of volume biomass per area of substratum obtained from biological quadruplicates with three technical replicates.

done on the basis of 12 images of each bacterial strain and the standard deviations were low, indicating that the biofilms were reproducible (Table 1).

Biofilms formed by the *P. aeruginosa* wild type and *fliM* mutant were carefully washed to remove planktonic bacteria, and subsequently, PMNs were added and the oxidative-burst response of the PMNs was assessed. As shown in Fig. 1 (middle graphs), the temporal development of the PMN response differed for the wild type and *fliM* biofilms, but the strengths of the responses were similar. The strengths of the PMN responses were not significantly different (Fig. 2A and Table S2), but the times to the peak of the oxidative burst differed significantly between the wild type and the *fliM* biofilm, with the PMNs responding faster against the *fliM* biofilm (Fig. 2B and Table S2). The faster recognition of the *fliM* mutant biofilm was unexpected but may be a result of the minor structural differences between the biofilms despite their identical extracellular matrices. Together, these results indicate that the presence of flagella is not a prerequisite for activation of a PMN response against biofilms.

We complemented the *fliM* mutation by insertion of the *fliM* gene in the ϕCTX integration site of the *P. aeruginosa fliM* mutant bacteria, and we found that the response of the PMNs to the complemented strain was similar to the response of the PMNs to the wild type (Fig. S1).

***P. aeruginosa* biofilms with distinct polysaccharide matrices elicit distinct PMN responses.** We subsequently focused on other aspects of the *P. aeruginosa* biofilm that could influence the immune response. Exopolysaccharides are key matrix components of biofilms formed by various bacterial species, including *P. aeruginosa*, of which the PAO1 strain employed in the current study can produce Pel, Psl, and alginate. To dissect the involvement of each of the polysaccharides in the response of PMNs against *P. aeruginosa* biofilms, we created an array of mutants overproducing only one of the exopolysaccharides while being deficient in synthesis of the remaining two (Table 2). Additionally, alginate-producing strains with a reinforced biofilm matrix resulting from concomitant overproduction of Pel or Psl were also created (Table 2). For Pel and Psl, overproduction of the exopolysaccharides was made possible by exchanging the *pelA* and *pslA* promoters, respectively, with an *araC-Pbad* cassette enabling arabinose-inducible overexpression of the biosynthesis operons (32, 33). For alginate, overproduction of the polysaccharide was enabled by exchanging *mucA* with the *mucA22* allele. The *mucA22* allele is found among mucoid clinical isolates and causes translation of a degenerate version of the anti-sigma factor MucA (34). This, in turn, deregulates the

TABLE 2 List of polysaccharide mutants and their denotation[a]

Strain name	Denotation in text
PAO1	PAO1
Pbad-pel Δ*psl* Δ*alg*	Pel^+ (Psl^- Alg^-)
Pbad-psl Δ*pel* Δ*alg*	Psl^+ (Pel^- Alg^-)
mucA22 Δ*pel* Δ*psl*	Alg^+ (Pel^- Psl^-)
mucA22 Pbad-pel Δ*psl*	Alg^+ Pel^+ (Psl^-)
mucA22 Pbad-psl Δ*pel*	Alg^+ Psl^+ (Pel^-)

[a]See Table 3 for details on the genotypes.

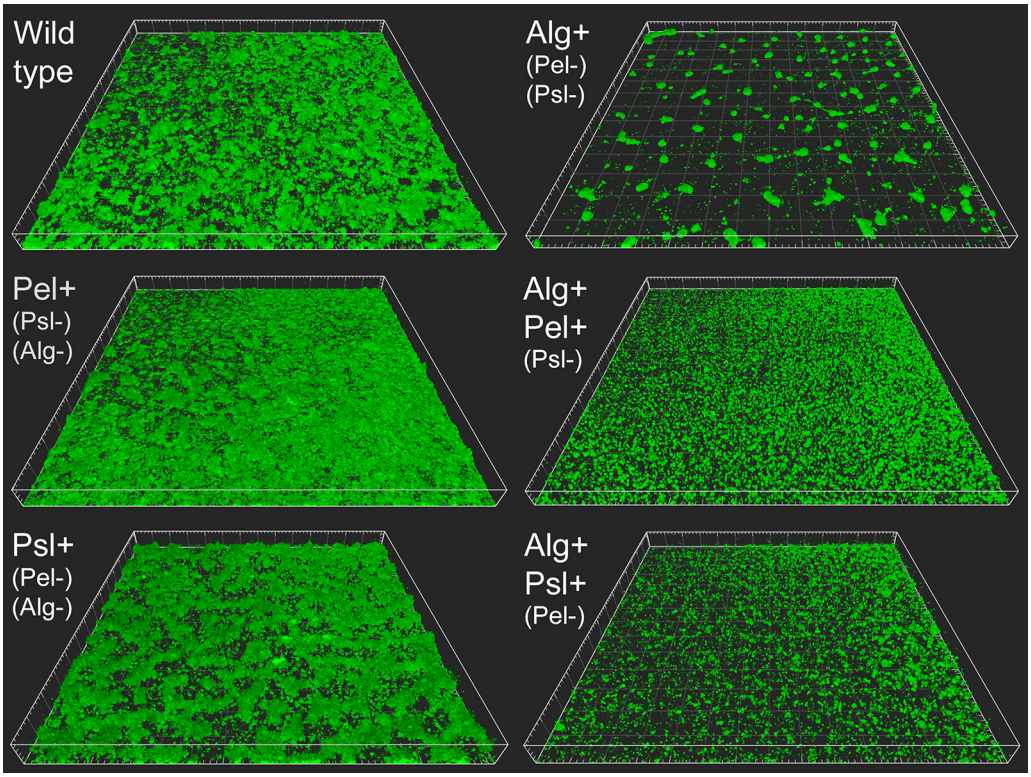

FIG 4 Biofilms formed by the *P. aeruginosa* PAO1 wild type and matrix exopolysaccharide mutants at the bottoms of microplate wells. Biofilms were established under static conditions for 24 h at 37°C, subsequently washed to remove planktonic cells, and stained with the green fluorescent dye Syto9 for visualization. Images displayed are 3D projections of image stacks captured using confocal laser scanning microscopy and a 20×/0.8 air objective. Grid size is 50 μm.

sigma factor AlgU (σ22), causing constitutive overexpression of the alginate biosynthesis operon via the *algD* promoter (35). Measurements of the growth rate of the wild type and the various mutants used in this study indicated that the strains grew equally well (Fig. S2).

We cultivated biofilms of the *P. aeruginosa* wild type and the different polysaccharide mutants at the bottoms of microplates. Compared to the wild-type biofilm, the majority of the mutant biofilms displayed a similar or slightly reduced amount of biomass (Fig. 4 and Table 1). In contrast, the mutant that produced only alginate formed biofilms with less biomass than that of the wild-type biofilm (Fig. 4 and Table 1). The biofilm of the alginate-only strain was composed of discrete microcolonies with large voids almost devoid of bacteria (Fig. 4). The two strains that produced Pel or Psl together with alginate did not form the isolated microcolonies observed for the alginate-only strain but instead formed biofilms composed of small clusters of cells evenly scattered across the surface (Fig. 4). The differences in structure and biomass between the various polysaccharide mutants indicated that the exopolysaccharides played a strong role in the development of biofilms, as expected.

PMNs were added to biofilms of the matrix polysaccharide mutants, and luminol-enhanced chemiluminescence was used to record their oxidative-burst response. The response of the PMNs was dependent on the type of polysaccharide constituting the biofilm matrix (Fig. 5 and 6). When the PMNs encountered a biofilm with a polysaccharide matrix consisting of a combination of alginate and Psl, they responded vigorously and swiftly (Fig. 5 and 6). Compared to the other type of biofilm matrices tested, the response toward the biofilm with an alginate/Psl-rich matrix was significantly increased both in terms of the strength of the response and in terms of the response kinetics (see Tables S3 and S4 for complete comparative statistics). Neither biofilm with a matrix comprised solely of alginate nor Psl induced the same vigorous PMN response,

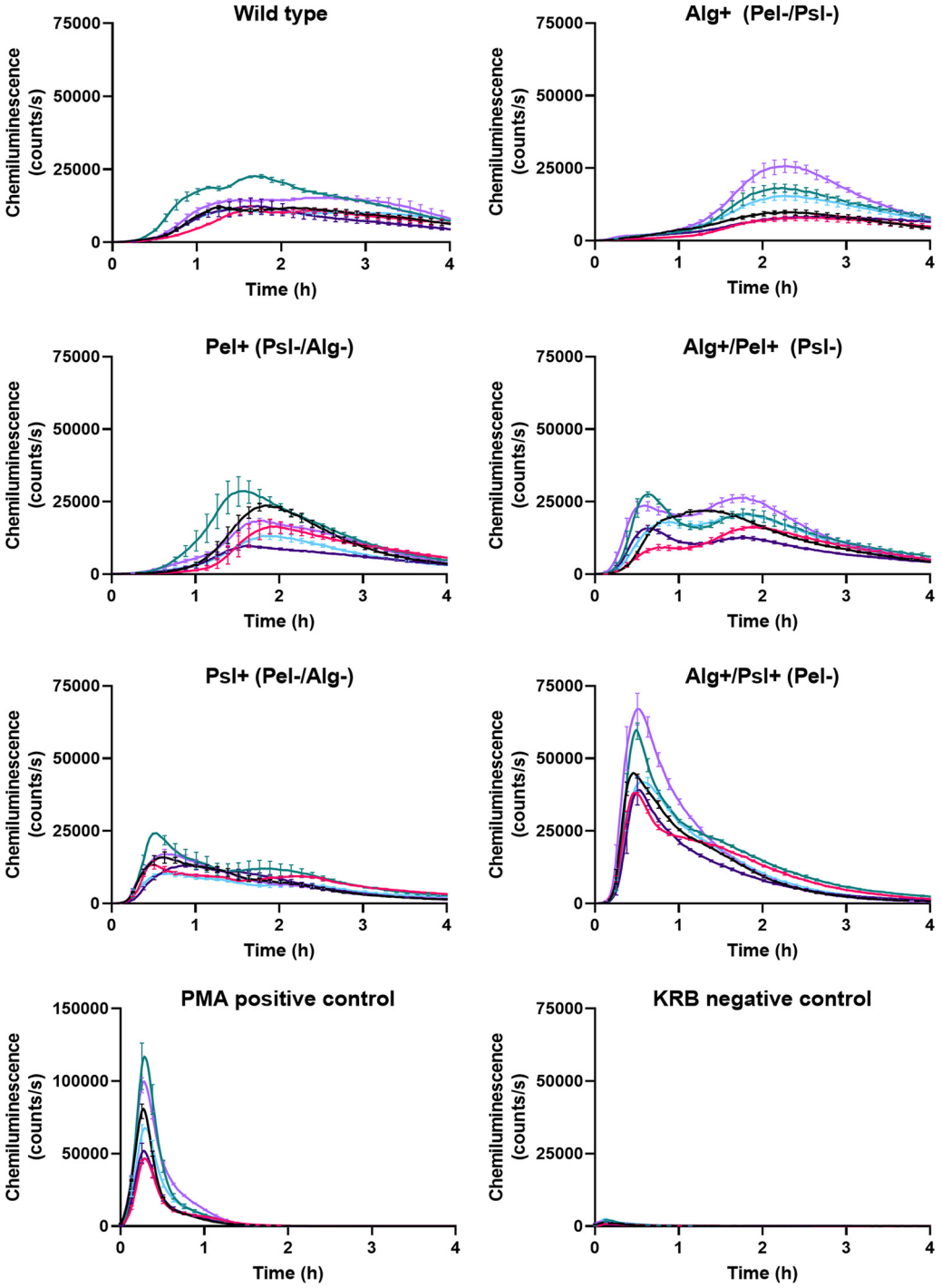

FIG 5 Oxidative-burst response of PMNs toward biofilms of the *P. aeruginosa* PAO1 wild type and matrix polysaccharide mutants. The biofilms were grown in microplate wells and were subsequently washed carefully to remove planktonic cells before PMNs were added at time zero. Luminol-enhanced chemiluminescence was used as a measure of the oxidative burst of PMNs. PMA was used as a positive control of reactive oxygen species release by the PMNs. Krebs-Ringer buffer supplemented with 10 mM glucose (KRB) was used as a negative control. PMNs were purified from the blood of healthy human volunteers. Complete chemiluminescence curves from six donors are shown as averages of three technical replicates. Note the individual *y* axis value chosen for the positive control. Error bars indicate standard deviations.

indicating that the PMNs responded specifically to the alginate/Psl combination. Despite their identical structures and amounts of attached biomass, the PMN responses also differed significantly between the alginate/Psl-rich biofilm and the alginate/Pel-rich biofilm ($P < 0.05$). This observation strengthened the notion of the alginate/Psl

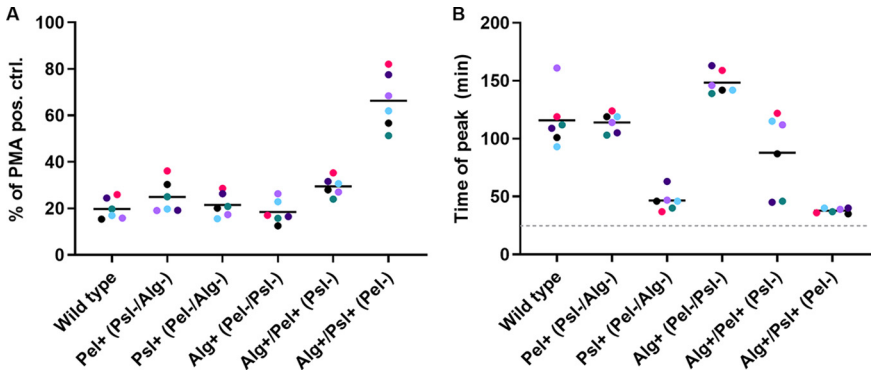

FIG 6 Parameters characterizing the oxidative-burst response of PMNs toward the *P. aeruginosa* PAO1 wild type and matrix polysaccharide mutants. The parameters are derived from the chemiluminescence curves shown in Fig. 1. (A) Peak chemiluminescence levels normalized to those of cells incubated with the positive control PMA. (B) Time point of the peak chemiluminescence level. The dashed gray line shows the average peak time of the PMA-stimulated positive controls. Symbol color indicates the individual donors ($n = 6$). Data points shown for each donor are the averages of three technical replicates. The horizontal bar indicates the mean across all donors.

matrix combination provoking a specific and vigorous response from the innate immune system. However, it should be noted that the PMNs also responded quickly toward the biofilm with a matrix comprised solely of Psl (Fig. 6), which indicates that this polysaccharide alone has the ability to trigger a fast release of ROS from the PMNs upon contact.

Finally, to corroborate the results of the oxidative burst against the different biofilms, degranulation levels of the primary antibacterial granules were quantified. This was accomplished by analyzing the concentration of myeloperoxidase released into the supernatant upon completion of the oxidative-burst measurements after 4 h of challenge. The release of myeloperoxidase was found to be increased for PMNs exposed to the alginate/Psl-rich biofilm matrix as well as the Psl-rich biofilm matrix (Fig. 7), although only the difference in degranulation between PMNs exposed to the alginate-rich biofilm matrix and the alginate/Psl-rich biofilm matrix was statistically significant ($P < 0.05$; see Table S5 for complete comparative statistics). This was in accordance with the results of the oxidative-burst assessments (Fig. 6), indicating a generally increased immune response of PMNs that encounter a biofilm rich in alginate and Psl exopolysaccharides. We also quantified PMN degranulation levels elicited by biofilms formed

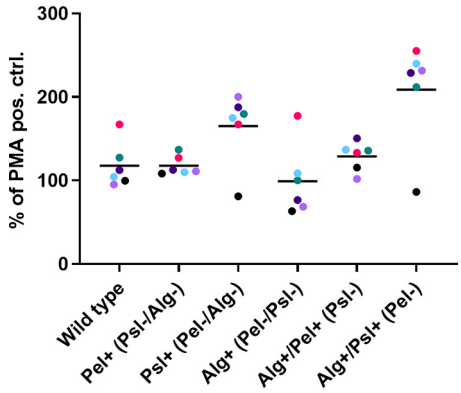

FIG 7 Levels of myeloperoxidase degranulation marker after challenge of PMNs with biofilms of *P. aeruginosa* PAO1 wild type and matrix polysaccharide mutants. Levels of myeloperoxidase released from degranulation of primary granules were normalized to PMA positive controls. Protein levels in the supernatant were measured upon completion of the oxidative-burst assay (after 4 h of challenge). Symbol color indicates the individual donors ($n = 6$). Data points shown for each donor are the averages of three technical replicates. The horizontal bar indicates the mean across all donors.

by the nonflagellated *fliM* mutant in comparison to wild-type biofilms. As shown in Fig. S3, the release of myeloperoxidase was found to be increased for PMNs exposed to the *fliM* mutant biofilms compared to wild-type biofilms. This supports the conclusion that flagella are not a prerequisite for the response of PMNs to *P. aeruginosa* biofilms.

DISCUSSION

The current study was conducted to investigate the response of immune cells to components of the *P. aeruginosa* biofilm matrix in a biofilm context. Previous studies have investigated the response of immune cells to purified components of the *P. aeruginosa* biofilm matrix. Ramirez et al. (29) investigated the inflammatory potential of exopolysaccharides isolated from biofilms of *P. aeruginosa* PAO1. Because this bacterial strain does not produce significant amounts of alginate (36), these polysaccharides were most likely Psl and Pel. The authors found that the exopolysaccharides elicited a higher inflammatory response from macrophages than bacterial extracellular DNA. Ciszek-Lenda et al. (28) investigated the response of phagocytes to spend medium of biofilm cultures of a mucoid *P. aeruginosa* strain. In this case the majority of the isolated exopolysaccharide was most likely alginate. It was found that the polysaccharide elicited a low inflammatory response from phagocytes compared to the inflammatory response elicited by bacterial extracellular DNA. However, the authors argued that the concentration of exopolysaccharide in their experiments likely was much lower than that found in *P. aeruginosa* biofilm infections. Pestrak et al. (27) investigated the response of PMNs to purified Psl and Pel, and they found that exposure to the individual exopolysaccharides did not stimulate ROS production by the PMNs. Since the immunogenic potential of biofilm matrix components may be different in a biofilm context than in a purified form, we found it of interest to investigate the response of immune cells to components of the *P. aeruginosa* biofilm matrix in a biofilm context.

In the initial part of the study, we investigated if classical PAMPs play a role in the activation of PMNs by *P. aeruginosa* biofilms. The polar flagellum of *P. aeruginosa*—and in part the motility conferred by the appendage—has been shown to be important for recognition of the bacterium by the innate immune system and for nonopsonic phagocytosis by macrophages and PMNs (25, 37, 38). This was confirmed in this study when PMNs were exposed to planktonic cultures of *P. aeruginosa* PAO1 and an isogenic flagellum-deficient *fliM* mutant. During biofilm formation, however, flagella may be physically shielded and obstructed in their movement by the extracellular matrix. We therefore hypothesized that the immunostimulatory capacity of the flagellum is less pronounced—or absent—when *P. aeruginosa* is grown as a biofilm. In accordance, our experiments with biofilms of the *P. aeruginosa* wild type and a flagellum-deficient mutant indicated that flagella do not play a major role in the PMN response to biofilms. This is in accordance with flagellum synthesis and functionality being downregulated in clinically relevant mucoid and RSCV strains of *P. aeruginosa* that still elicit a detrimental immune response (17, 39). Also, while the inflammatory response persists, there is a selection for nonmotile mutants during chronic infections, such as that of the CF lung (37).

Since the extracellular biofilm matrix is exposed to immune cells, and polysaccharides constitute a substantial part of the *P. aeruginosa* biofilm matrix, we hypothesized that the polysaccharides play a role in the response of PMNs to *P. aeruginosa* biofilms. Thus, we investigated the response of PMNs to *P. aeruginosa* biofilms that displayed various kinds of polysaccharide matrices. The biofilm exopolysaccharide matrix had a significant impact on the oxidative-burst response of the PMNs. A matrix made up of a combination of alginate and Psl provoked the PMNs to produce a very swift and vigorous response compared to a matrix made up of either polysaccharide alone, in terms of both the oxidative burst and degranulation of the primary granules responsible for release of antimicrobial compounds.

At present, we do not know the mechanism behind the increased activation of the PMNs when encountering an alginate- and Psl-rich biofilm. One explanation is that the overall biofilm landscape that the PMNs encountered in this study is especially efficient

in triggering the PMNs. That it matters what the PMNs "see" of the biofilm has recently been put forward by others (40). The different exopolysaccharide mutants formed different biofilm structures, in accordance with previous work (10, 33, 41, 42). The exact structure of the alginate- and Psl-rich biofilm matrix might provide the possibility of the PMNs coming into close contact with the bacteria, and although unable to efficiently phagocytose them, the PMNs may still be provoked to respond. Such a strong immune response, e.g., the expulsion of neutrophil extracellular traps or release of ROS in spite of reduced phagocytosis, is well described (27, 43). However, in the case of the alginate/Psl-rich and the alginate/Pel-rich biofilms, we observed an overall structural similarity, yet the strengths of the PMN oxidative-burst response were very different for the two types of biofilm. This indicates that the molecular structure or chemical properties of the individual matrix constituents also play a significant role in activating the PMNs. A dominant factor discriminating the two types of biofilm matrices might be the Psl polysaccharide. Psl has been shown to afford increased contact between *P. aeruginosa* and epithelial cells with a subsequent activation of the cells and has also been implicated in macrophage activation by Psl-overproducing RSCVs (27, 44). As such, the differences between Pel and Psl might cause a strong PMN activation against the alginate/Psl-rich biofilm but not against the alginate/Pel-rich biofilm. In contrast to the strength of the PMN response, there was no significant difference between the timing of the peak response against the alginate/Psl-rich biofilm and the alginate/Pel-rich biofilms. However, the difference in peak response between the Psl-rich and Pel-rich biofilms was significant, indicating that Psl but not alginate plays a role in the swiftness of the PMN response against biofilm of *P. aeruginosa*.

The luminol-enhanced chemiluminescence detection method used in this study affords detection of both the extracellular and intracellular (intraphagosomal) oxidative burst (45). However, considering the decreased phagocytosis of biofilm bacteria (18, 46, 47), the majority of the signal detected likely originates from an extracellular oxidative burst.

The ability of *P. aeruginosa* biofilm to activate the complement system may have a significant impact on the innate immune response against biofilm, since opsonization with C3 fragments engages complement receptors on the PMNs. However, allowing complement opsonization of the biofilm may confound the response against matrix exopolysaccharide, since opsonization mainly occurs on LPS (48). Therefore, no serum was added during incubation in the present study, and determination of the significance of serum components on the immune response against matrix exopolysaccharides of biofilm awaits further studies.

Our study is based on *P. aeruginosa* strains that are genetically modified in the laboratory, and the clinical relevance of the strains may be questioned. However, evidence has been presented that Psl protects *P. aeruginosa* from host defenses within the CF lung prior to their conversion to the alginate-overproducing mucoid phenotype (22). Thus, it is possible that an extracellular biofilm matrix dominated by Psl is important in the initial stage of chronic lung infection before the bacteria mutate to produce a biofilm matrix dominated by alginate. In addition, evidence has been provided that Psl produced by mucoid *P. aeruginosa* play an important role in the establishment of biofilms (11). Therefore, *P. aeruginosa* strains that produce both Psl and alginate may be particularly clinically relevant. Moreover, *P. aeruginosa* strains that overproduce Psl and Pel are of clinical relevance since these RSCVs are frequently isolated from infections (15–17).

The results presented here add to the discussion of how immune cells perceive and respond to biofilms. Using our array of *P. aeruginosa* matrix exopolysaccharide mutants, we found that the nature of the biofilm matrix is important for the PMN response and that distinct combinations of matrix components significantly enhance the immunostimulatory effect of the biofilm. A matrix composed of Psl and alginate elicits a particularly strong oxidative-burst response from approaching PMNs. This polysaccharide combination is of high clinical relevance, as the capacity to produce alginate and Psl is common to many isolates from the lungs of CF patients (11). Thus, this polysac-

TABLE 3 List of strains and plasmids used in this study

Strain or plasmid	Description	Source and/or reference
E. coli strains		
DH5α	Standard cloning strain	Lab collection
HB101	Standard cloning strain	Lab collection
MS690	MG1655 Δ*hsdR*; cloning strain	Mark A. Schembri
P. aeruginosa strains		
PAO1	Wild type	Lab collection, 57
Δ*fliM*	*fliM* deletion mutant; flagellum deficient	This study
Δ*pel*	*pelA* deletion mutant; Pel deficient	58
Δ*psl*	*pslBCD* deletion mutant; Psl deficient	58
Δ*pel* Δ*psl*	*pelA* and *pslBCD* double deletion mutant; Pel and Psl deficient	58
Δ*pel* Δ*alg*	*pelA* and *algD* double deletion mutant; Pel and alginate deficient	This study
Δ*psl* Δ*alg*	*pslBCD* and *algD* double deletion mutant; Psl and alginate deficient	This study
Δ*pel* Δ*psl* Δ*alg*	*pelA*, *pslBCD* and *algD* triple deletion mutant; Pel, Psl, and alginate deficient	59
Δ*pel* Δ*alg Pbad*-Psl	*pelA* and *algD* double deletion mutant; Pel and alginate deficient. Native *pslA* promoter exchanged with *araC-Pbad*; inducible overproduction of Psl	This study
Δ*psl* Δ*alg Pbad*-Pel	*pslBCD* and *algD* double deletion mutant; Psl and alginate deficient. Native *pelA* promoter exchanged with *araC-Pbad*; inducible overproduction of Pel	This study
Δ*pel Pbad*-Psl *mucA22*	*pelA* deletion mutant; Pel deficient. Native *pslA* promoter exchanged with *araC-Pbad*; inducible overproduction of Psl. *mucA22* allele knock-in; overproduction of alginate; mucoid.	This study
Δ*psl Pbad*-Pel *mucA22*	*pslBCD* deletion mutant; Psl deficient. Native *pelA* promoter exchanged with araC-Pbad; Inducible overproduction of Pel. *mucA22* allele knock-in; overproduction of alginate; mucoid	This study
Δ*pel* Δ*psl mucA22*	*pelA* and *pslBCD* double deletion mutant; Pel and Psl deficient. *mucA22* allele knock-in; overproduction of alginate; mucoid.	This study
WT *gfp*	Wild type; tagged with miniTn7-gfp-gm; Gm^r	This study
Δ*fliM gfp*	Δ*fliM* tagged with mini-Tn7-gm; Gm^r	This study
Δ*pel* Δ*alg Pbad*-Psl *gfp*	Δ*pel* Δ*alg Pbad*-Psl; tagged with miniTn7-gfp-gm; Gm^r	This study
Δ*psl* Δ*alg Pbad*-Pel *gfp*	Δ*psl* Δ*alg Pbad*-Pel; tagged with miniTn7-gfp-gm; Gm^r	This study
Δ*pel Pbad*-Psl *mucA22 gfp*	Δ*pel Pbad*-Psl *mucA22*; tagged with miniTn7-gfp-gm; Gm^r	This study
Δ*psl Pbad*-Pel *mucA22 gfp*	Δ*psl Pbad*-Pel *mucA22*; tagged with miniTn7-gfp-gm; Gm^r	This study
Δ*pel* Δ*psl mucA22 gfp*	Δ*pel* Δ*psl mucA22*; tagged with miniTn7-gfp-gm; Gm^r	This study
FRD1	Clinical isolate; source of *mucA22* allele	34
Pbad-pel	Source of *araC-Pbad-pelA* fragment	32
WFPA801	Source of *araC-Pbad-pslA* fragment	33
Plasmids		
pENTR-fliM-KO	Allelic-exchange vector for in-frame deletion of *fliM*; Gm^r	This study
pENTR-algD-KO	Allelic-exchange vector for in-frame deletion of *algD*; Gm^r	59
pENTR-Pbad-pel-KI	Allelic-exchange vector for exchange of native *pelA* promoter with *araC-Pbad*; Gm^r	This study
pENTR-Pbad-psl-KI	Allelic-exchange vector for exchange of native *pslA* promoter with *araC-Pbad*; Gm^r	This study
pENTR-mucA22-KI	Allelic-exchange vector for knock-in of the *mucA22* allele; Gm^r	This study
pDONRPEX18Gm	Gateway donor vector allelic exchange vector creation; Gm^r	52
pBK-miniTn7-gfp2	Source of miniTn7-gfp-gm transposon for Gfp tagging; Gm^r (Ap^r)	53
pRK600	Mobilizing helper plasmid for triparental mating; Cm^r	60
pTNS1	Source of miniTn7 transposase genes; Ap^r	54

charide combination may be involved in provoking a substantial extracellular release of ROS that can be detrimental to the surrounding host tissue. Our work may stimulate more in-depth research aimed at elucidating the finer structural and biochemical details of the interplay between the biofilm matrix, the embedded bacteria, and the immune cells. This research could lay the groundwork for development of new treatment strategies aimed at modulating the immune response toward the recalcitrant and inflammatory biofilm-based infections.

MATERIALS AND METHODS

Bacterial strains and media. The bacterial strains and plasmids used in this study are listed in Table 3. Strains were routinely grown as liquid cultures in lysogeny broth (LB) and propagated on LB agar unless stated otherwise. AB minimal medium (49) supplemented with 10 μM $FeCl_3$ and 10 mM sodium citrate was used as the selective medium during conjugations. ABTrace minimal medium (50) supplemented with 0.2% (wt/vol) Casamino Acids, 1 μM $FeCl_3$, and 10 mM potassium nitrate was used as the

growth medium for microplate biofilms. Induction of gene expression was achieved by the addition of 0.2% (wt/vol) L-arabinose. For experiments involving isolated human PMNs, Krebs-Ringer balanced salt solution supplemented with 10 mM glucose (KRB) was used as the medium (51). Antibiotics were used as follows: for *Escherichia coli*, gentamicin was used at 15 μg/ml and chloramphenicol at 6 μg/ml; for *P. aeruginosa*, gentamicin was used at 100 μg/ml (for strain construction) and 50 μg/ml (for microplate biofilm formation).

Vector construction and strain creation. Allelic-exchange vectors based on the suicide vector pDONRPEX18Gm were constructed using the general guidelines of Hmelo et al. (52). Sequences of the primers used are listed in Table S6. pENTR-Pbad-pel-KI was constructed by subcloning the *araC-Pbad-pelA* promoter region from *P. aeruginosa* P_{BAD}pel (32) including upstream and downstream genomic regions to facilitate allelic exchange in the *P. aeruginosa* mutant strains originating from our lab. pENTR-Pbad-psl-KI was constructed in an identical manner by subcloning the *araC-Pbad-pslA* promoter region from *P. aeruginosa* P_{BAD}psl (33). pENTR-mucA22-KI was constructed by subcloning the *mucA*22 allele from *P. aeruginosa* FRD1 (34).

Allelic exchange in our *P. aeruginosa* PAO1 strains was facilitated by triparental mating between the recipient strains, the allelic-exchange vector donor strains and the pRK600 conjugation helper strain. Following isolation of transconjugants on minimal citrate medium, the merodiploid state was resolved by propagation on LB agar without salt, supplemented with 10% (wt/vol) sucrose. PCR was used to screen for candidates displaying the mutant genotype.

Tn*7*-Gfp-Gm tagging of the strains was conducted by simultaneous transformation of pBK-miniTn7-gfp2 (53) and pTNS1 (54) using the standard sucrose-based method for preparing competent cells (55). Fluorescence of the resulting transformants was verified using an epifluorescence microscope equipped with a filter for visualizing Gfp.

Microplate biofilm development. Biofilms of the various *P. aeruginosa* strains were established on the bottom surface of 96-well optical-bottom microplates (Nunc MicroWell; Thermo Fisher Scientific) based on the method described by Müsken et al. (56). Briefly, overnight cultures were diluted to an optical density at 600 nm (OD_{600}) of 0.02 in minimal medium and added to the microplate wells in volumes of 200 μl. Unused wells were filled with equal volumes of water. The plate was covered with a gas-permeable rayon membrane (Nunc, Thermo Fisher Scientific) and incubated statically at 37°C for 24 h in a humidified incubator. Plates with black and white well sides were used for microscopy and PMN treatments, respectively. For PMN treatments, the plates were made fully opaque and ready for chemiluminescence detection (see below) by attaching a white adhesive seal on the backs of the plates (BackSeal; Perkin Elmer).

After incubation, the microplates were very carefully washed to preserve the biofilms at the bottoms of the wells. Aspiration was done manually using a multipipette in a very slow and gentle manner with the pipette tips touching the well bottoms near the well edges in the same place during all aspirations. A total of 50 μl of supernatant was retained in the wells during the initial aspiration to keep the biofilms submerged and undisturbed. Subsequently, the wells were washed twice with 200 μl of 0.9% saline using an aspiration volume of same 200 μl. As for the aspiration steps, dispensing was done in a slow and gentle manner, taking care to reduce liquid turbulence that could otherwise disturb the biofilms. Finally, 200 μl of saline was added. For the PMN treatments, the plates were left at room temperature until the immune cells were ready. For microscopy, the final volume of saline added was supplemented with Syto9 (Molecular Probes, Thermo Fisher Scientific) diluted 800 times for fluorescent staining of the biofilms. Staining was done for approximately 1 h in the dark at room temperature.

Blood samples and purification of polymorphonuclear neutrophils. Heparinized whole-blood samples were obtained from healthy donors attending the Copenhagen University Hospital blood bank (Rigshospitalet, Copenhagen, Denmark). Donors were anonymous, with samples being marked only for age and gender. Due to the anonymity of the donors, the National Ethical Committee of Denmark waived the need for ethical approval of this study.

PMNs were purified from the heparinized whole-blood samples in the following way. Samples were mixed with a 5% (wt/vol) dextran solution and the erythrocytes were allowed to sediment for 60 to 90 min. The leukocyte-enriched plasma was then layered on top of Lymphoprep (STEMCELL Technologies) and centrifuged. The PMN-enriched pellet then underwent hypertonic treatment to lyse leftover erythrocytes. After a final centrifugation step, PMNs were resuspended in KRB.

The concentration of the purified PMNs was estimated using TruCount tubes (BD Biosciences) and a BD FacsCanto II flow cytometer (BD Biosciences) according to the manufacturer's description. KRB was used to dilute the PMNs to a final stock concentration of 3.3×10^6/ml.

PMN oxidative-burst assay. Luminol-enhanced chemiluminescence was used to evaluate the oxidative-burst response of PMNs exposed to microplate biofilms or planktonic bacteria. To prepare the preformed biofilms, the microplate wells were washed twice with 200 μl of KRB in the same manner as the aforementioned washes with saline.

The planktonic samples came from cultures grown under shaking conditions for 3.5 h at 37°C. The cultures were initially prepared by inoculating a standard overnight (ON) culture in ABTrace minimal medium supplemented with 1 μM $FeCl_3$ and 0.5% (wt/vol) Casamino Acids to an OD_{600} of 0.05. Subsequently, 500-μl samples were taken from the very top of the liquid culture column after they had been standing still for 5 min. This precaution minimized the risk of carryover of confounding biofilm-like aggregates by allowing them to sediment in the lower part of the liquid column. Samples were then diluted to an OD_{600} of 0.25 in KRB, and 50-μl volumes were added to the wells of the assay microplates. The amount of planktonic bacteria added corresponded to a multiplicity of infection of 50 bacteria per PMN.

As a negative control, 50 μl of KRB was added to empty wells. As a positive control, 50 μl of 35 μM PMA in KRB added to empty wells was used (final assay concentration, 7 μM).

The assay samples were subsequently completed by carefully adding 125 μl of KRB supplemented with 140 μM luminol (final assay concentration, 70 μM), followed by addition of 75 μl of purified PMNs (final assay concentration, 1×10^6 PMNs/ml). Finally, the assay plate was incubated at 37°C in a Victor X4 plate reader (Perkin Elmer) set for measuring chemiluminescence (counts per second). Measurement of the plate was repeated 99 times, with a 40-s interval between repeats for a total assay duration of 4 h.

Visualization and quantification of biofilms. Confocal laser scanning microscopy was used to visualize the microplate biofilms to which the PMNs were exposed. Initially, biofilm-containing wells of the microplates were washed twice with KRB in addition to the aforementioned washes with saline. Finally, 200-μl volumes of KRB were added to the wells. Image stacks of the biofilms were acquired using a Zeiss LSM880 microscope equipped with a 20×/0.8 air objective set for detecting Syto9. Postacquisition processing of the image stacks for publication was done using Imaris image analysis software (Bitplane; Oxford Instruments).

For quantification of the biofilms, image stacks were acquired at three random positions (technical triplicates) in four microplate wells (biological quadruplicates) for each strain. To quantify the biomass in individual image stacks, an isosurface covering the biomass was generated using constant parameters between images and strains. Smoothing was enabled and automatically set, background was automatically eliminated, and the lower signal intensity threshold was set to 5. The volume of biomass (i.e., the volumes of the calculated isosurface structures) was obtained using the Measurement Pro package for Imaris image analysis software. Data are presented as biomass volume (cubic micrometers) per area of substratum (square micrometers).

PMN degranulation analysis. Primary granule degranulation levels of PMNs exposed to bacterial biofilms were measured as follows. Immediately upon completion of the oxidative-burst assay, the microplate was centrifuged at 1,000 × *g* for 10 min to pellet the PMNs. A total of 150 μl of supernatant from each well was then transferred to the corresponding well of a filter plate equipped with a 0.22-μm hydrophilic polyvinylidene fluoride low-protein-binding membrane (Millipore MultiScreen$_{HTS}$ GV; Merck). The supernatants were sterile filtered into a collection plate by centrifugation at 1,000 × *g* for 2 min and kept frozen at −80°C until analysis.

The level of myeloperoxidase degranulation marker was measured on 50-fold-diluted supernatants using the Luminex Bio-Plex 200 system (Bio-Rad Laboratories) and a myeloperoxidase-specific assay (human magnetic Luminex assay; R&D Systems) according to the manufacturers' instructions.

Data presentation and statistical analysis. Graphical presentation and statistical analysis of the data included in the study were conducted using Prism 8 (GraphPad Software). To minimize donor-to-donor variation, the result of the positive PMA control for each donor was used to normalize the data for the statistical analysis of the variables used to describe the oxidative-burst response of PMNs as well as for the degranulation analysis. The differences between groups were compared using a one-way repeated-measures analysis of variance (ANOVA) pairing responses from the same donor. Geisser-Greenhouse correction was applied and Tukey's multiple-comparison test was used to compare the mean of each strain with the mean of every other strain. A *P* level of 0.05 was considered significant.

SUPPLEMENTAL MATERIAL

Supplemental material is available online only.

SUPPLEMENTAL FILE 1, PDF file, 0.7 MB.

ACKNOWLEDGMENTS

We thank Pia Grothe Meincke for technical assistance with the Luminex assay. We acknowledge Kasper Nørskov Kragh for assistance with the biofilm quantification.

This study was funded by a grant from the Danish Council for Independent Research (DFF-7016-00039) to Tim Tolker-Nielsen.

REFERENCES

1. Del Pozo JL. 2018. Biofilm-related disease. Expert Rev Anti Infect Ther 16:51–65. https://doi.org/10.1080/14787210.2018.1417036.
2. Burmolle M, Thomsen TR, Fazli M, Dige I, Christensen L, Homoe P, Tvede M, Nyvad B, Tolker-Nielsen T, Givskov M, Moser C, Kirketerp-Moller K, Johansen HK, Hoiby N, Jensen PO, Sorensen SJ, Bjarnsholt T. 2010. Biofilms in chronic infections—a matter of opportunity—monospecies biofilms in multispecies infections. FEMS Immunol Med Microbiol 59:324–336. https://doi.org/10.1111/j.1574-695X.2010.00714.x.
3. Nauseef WM. 2007. How human neutrophils kill and degrade microbes: an integrated view. Immunol Rev 219:88–102. https://doi.org/10.1111/j.1600-065X.2007.00550.x.
4. Rada B. 2017. Interactions between neutrophils and Pseudomonas aeruginosa in cystic fibrosis. Pathogens 6:10. https://doi.org/10.3390/pathogens6010010.
5. Jensen PO, Givskov M, Bjarnsholt T, Moser C. 2010. The immune system vs. Pseudomonas aeruginosa biofilms. FEMS Immunol Med Microbiol 59:292–305. https://doi.org/10.1111/j.1574-695X.2010.00706.x.
6. Tolker-Nielsen T. 2014. Pseudomonas aeruginosa biofilm infections: from molecular biofilm biology to new treatment possibilities. APMIS Suppl 122:1–51. https://doi.org/10.1111/apm.12335.
7. Jennings LK, Storek KM, Ledvina HE, Coulon C, Marmont LS, Sadovskaya I, Secor PR, Tseng BS, Scian M, Filloux A, Wozniak DJ, Howell PL, Parsek MR. 2015. Pel is a cationic exopolysaccharide that cross-links extracellular DNA in the Pseudomonas aeruginosa biofilm matrix. Proc Natl Acad Sci U S A 112:11353–11358. https://doi.org/10.1073/pnas.1503058112.
8. Byrd MS, Sadovskaya I, Vinogradov E, Lu H, Sprinkle AB, Richardson SH, Ma L, Ralston B, Parsek MR, Anderson EM, Lam JS, Wozniak DJ. 2009. Genetic and biochemical analyses of the Pseudomonas aeruginosa Psl

exopolysaccharide reveal overlapping roles for polysaccharide synthesis enzymes in Psl and LPS production. Mol Microbiol 73:622–638. https://doi.org/10.1111/j.1365-2958.2009.06795.x.
9. Franklin MJ, Nivens DE, Weadge JT, Howell PL. 2011. Biosynthesis of the Pseudomonas aeruginosa extracellular polysaccharides, alginate, Pel, and Psl. Front Microbiol 2:167. https://doi.org/10.3389/fmicb.2011.00167.
10. Colvin KM, Irie Y, Tart CS, Urbano R, Whitney JC, Ryder C, Howell PL, Wozniak DJ, Parsek MR. 2012. The Pel and Psl polysaccharides provide Pseudomonas aeruginosa structural redundancy within the biofilm matrix. Environ Microbiol 14:1913–1928. https://doi.org/10.1111/j.1462-2920.2011.02657.x.
11. Jones CJ, Wozniak DJ. 2017. Psl produced by mucoid Pseudomonas aeruginosa contributes to the establishment of biofilms and immune evasion. mBio 8:e00864-17. https://doi.org/10.1128/mBio.00864-17.
12. Fazli M, Almblad H, Rybtke ML, Givskov M, Eberl L, Tolker-Nielsen T. 2014. Regulation of biofilm formation in Pseudomonas and Burkholderia species. Environ Microbiol 16:1961–1981. https://doi.org/10.1111/1462-2920.12448.
13. Govan JR, Deretic V. 1996. Microbial pathogenesis in cystic fibrosis: mucoid Pseudomonas aeruginosa and Burkholderia cepacia. Microbiol Rev 60:539–574. https://doi.org/10.1128/MMBR.60.3.539-574.1996.
14. Mathee K, Ciofu O, Sternberg C, Lindum PW, Campbell JI, Jensen P, Johnsen AH, Givskov M, Ohman DE, Molin S, Hoiby N, Kharazmi A. 1999. Mucoid conversion of Pseudomonas aeruginosa by hydrogen peroxide: a mechanism for virulence activation in the cystic fibrosis lung. Microbiology 145:1349–1357. https://doi.org/10.1099/13500872-145-6-1349.
15. Evans TJ. 2015. Small colony variants of Pseudomonas aeruginosa in chronic bacterial infection of the lung in cystic fibrosis. Future Microbiol 10:231–239. https://doi.org/10.2217/fmb.14.107.
16. Malone JG, Jaeger T, Spangler C, Ritz D, Spang A, Arrieumerlou C, Kaever V, Landmann R, Jenal U. 2010. YfiBNR mediates cyclic di-GMP dependent small colony variant formation and persistence in Pseudomonas aeruginosa. PLoS Pathog 6:e1000804. https://doi.org/10.1371/journal.ppat.1000804.
17. Starkey M, Hickman JH, Ma L, Zhang N, De Long S, Hinz A, Palacios S, Manoil C, Kirisits MJ, Starner TD, Wozniak DJ, Harwood CS, Parsek MR. 2009. Pseudomonas aeruginosa rugose small-colony variants have adaptations that likely promote persistence in the cystic fibrosis lung. J Bacteriol 191:3492–3503. https://doi.org/10.1128/JB.00119-09.
18. Cabral DA, Loh BA, Speert DP. 1987. Mucoid Pseudomonas aeruginosa resists nonopsonic phagocytosis by human neutrophils and macrophages. Pediatr Res 22:429–431. https://doi.org/10.1203/00006450-198710000-00013.
19. Leid JG, Willson CJ, Shirtliff ME, Hassett DJ, Parsek MR, Jeffers AK. 2005. The exopolysaccharide alginate protects Pseudomonas aeruginosa biofilm bacteria from IFN-gamma-mediated macrophage killing. J Immunol 175:7512–7518. https://doi.org/10.4049/jimmunol.175.11.7512.
20. Learn DB, Brestel EP, Seetharama S. 1987. Hypochlorite scavenging by Pseudomonas aeruginosa alginate. Infect Immun 55:1813–1818. https://doi.org/10.1128/IAI.55.8.1813-1818.1987.
21. Simpson JA, Smith SE, Dean RT. 1989. Scavenging by alginate of free radicals released by macrophages. Free Radic Biol Med 6:347–353. https://doi.org/10.1016/0891-5849(89)90078-6.
22. Mishra M, Byrd MS, Sergeant S, Azad AK, Parsek MR, McPhail L, Schlesinger LS, Wozniak DJ. 2012. Pseudomonas aeruginosa Psl polysaccharide reduces neutrophil phagocytosis and the oxidative response by limiting complement-mediated opsonization. Cell Microbiol 14:95–106. https://doi.org/10.1111/j.1462-5822.2011.01704.x.
23. Lavoie EG, Wangdi T, Kazmierczak BI. 2011. Innate immune responses to Pseudomonas aeruginosa infection. Microbes Infect 13:1133–1145. https://doi.org/10.1016/j.micinf.2011.07.011.
24. Raoust E, Balloy V, Garcia-Verdugo I, Touqui L, Ramphal R, Chignard M. 2009. Pseudomonas aeruginosa LPS or flagellin are sufficient to activate TLR-dependent signaling in murine alveolar macrophages and airway epithelial cells. PLoS One 4:e7259. https://doi.org/10.1371/journal.pone.0007259.
25. Amiel E, Lovewell RR, O'Toole GA, Hogan DA, Berwin B. 2010. Pseudomonas aeruginosa evasion of phagocytosis is mediated by loss of swimming motility and is independent of flagellum expression. Infect Immun 78:2937–2945. https://doi.org/10.1128/IAI.00144-10.
26. Meluleni GJ, Grout M, Evans DJ, Pier GB. 1995. Mucoid Pseudomonas aeruginosa growing in a biofilm in vitro are killed by opsonic antibodies to the mucoid exopolysaccharide capsule but not by antibodies produced during chronic lung infection in cystic fibrosis patients. J Immunol 155:2029–2038.
27. Pestrak MJ, Chaney SB, Eggleston HC, Dellos-Nolan S, Dixit S, Mathew-Steiner SS, Roy S, Parsek MR, Sen CK, Wozniak DJ. 2018. Pseudomonas aeruginosa rugose small-colony variants evade host clearance, are hyper-inflammatory, and persist in multiple host environments. PLoS Pathog 14:e1006842. https://doi.org/10.1371/journal.ppat.1006842.
28. Ciszek-Lenda M, Strus M, Walczewska M, Majka G, Machul-Żwirbla A, Mikołajczyk D, Górska S, Gamian A, Chain B, Marcinkiewicz J. 2019. Pseudomonas aeruginosa biofilm is a potent inducer of phagocyte hyperinflammation. Inflamm Res 68:397–413. https://doi.org/10.1007/s00011-019-01227-x.
29. Ramirez T, Shrestha A, Kishen A. 2019. Inflammatory potential of monospecies biofilm matrix components. Int Endod J 52:1020–1027. https://doi.org/10.1111/iej.13093.
30. Barken KB, Pamp SJ, Yang L, Gjermansen M, Bertrand JJ, Klausen M, Givskov M, Whitchurch CB, Engel JN, Tolker-Nielsen T. 2008. Roles of type IV pili, flagellum-mediated motility and extracellular DNA in the formation of mature multicellular structures in Pseudomonas aeruginosa biofilms. Environ Microbiol 10:2331–2343. https://doi.org/10.1111/j.1462-2920.2008.01658.x.
31. Tolker-Nielsen T. 2015. Biofilm development. Microbiol Spectr 3:MB-0001-2014. https://doi.org/10.1128/microbiolspec.MB-0001-2014.
32. Colvin KM, Gordon VD, Murakami K, Borlee BR, Wozniak DJ, Wong GC, Parsek MR. 2011. The Pel polysaccharide can serve a structural and protective role in the biofilm matrix of Pseudomonas aeruginosa. PLoS Pathog 7:e1001264. https://doi.org/10.1371/journal.ppat.1001264.
33. Ma L, Jackson KD, Landry RM, Parsek MR, Wozniak DJ. 2006. Analysis of Pseudomonas aeruginosa conditional Psl variants reveals roles for the Psl polysaccharide in adhesion and maintaining biofilm structure postattachment. J Bacteriol 188:8213–8221. https://doi.org/10.1128/JB.01202-06.
34. Ohman DE, Chakrabarty AM. 1981. Genetic mapping of chromosomal determinants for the production of the exopolysaccharide alginate in a Pseudomonas aeruginosa cystic fibrosis isolate. Infect Immun 33:142–148. https://doi.org/10.1128/IAI.33.1.142-148.1981.
35. Hay ID, Wang Y, Moradali MF, Rehman ZU, Rehm BH. 2014. Genetics and regulation of bacterial alginate production. Environ Microbiol 16:2997–3011. https://doi.org/10.1111/1462-2920.12389.
36. Wozniak DJ, Wyckoff TJ, Starkey M, Keyser R, Azadi P, O'Toole GA, Parsek MR. 2003. Alginate is not a significant component of the extracellular polysaccharide matrix of PA14 and PAO1 Pseudomonas aeruginosa biofilms. Proc Natl Acad Sci U S A 100:7907–7912. https://doi.org/10.1073/pnas.1231792100.
37. Mahenthiralingam E, Campbell ME, Speert DP. 1994. Nonmotility and phagocytic resistance of Pseudomonas aeruginosa isolates from chronically colonized patients with cystic fibrosis. Infect Immun 62:596–605. https://doi.org/10.1128/IAI.62.2.596-605.1994.
38. Mahenthiralingam E, Speert DP. 1995. Nonopsonic phagocytosis of Pseudomonas aeruginosa by macrophages and polymorphonuclear leukocytes requires the presence of the bacterial flagellum. Infect Immun 63:4519–4523. https://doi.org/10.1128/IAI.63.11.4519-4523.1995.
39. Tart AH, Wolfgang MC, Wozniak DJ. 2005. The alternative sigma factor AlgT represses Pseudomonas aeruginosa flagellum biosynthesis by inhibiting expression of fleQ. J Bacteriol 187:7955–7962. https://doi.org/10.1128/JB.187.23.7955-7962.2005.
40. Watters C, Fleming D, Bishop D, Rumbaugh KP. 2016. Host responses to biofilm. Prog Mol Biol Transl Sci 142:193–239. https://doi.org/10.1016/bs.pmbts.2016.05.007.
41. Yang L, Hu Y, Liu Y, Zhang J, Ulstrup J, Molin S. 2011. Distinct roles of extracellular polymeric substances in Pseudomonas aeruginosa biofilm development. Environ Microbiol 13:1705–1717. https://doi.org/10.1111/j.1462-2920.2011.02503.x.
42. Ma L, Wang S, Wang D, Parsek MR, Wozniak DJ. 2012. The roles of biofilm matrix polysaccharide Psl in mucoid Pseudomonas aeruginosa biofilms. FEMS Immunol Med Microbiol 65:377–380. https://doi.org/10.1111/j.1574-695X.2012.00934.x.
43. Branzk N, Lubojemska A, Hardison SE, Wang Q, Gutierrez MG, Brown GD, Papayannopoulos V. 2014. Neutrophils sense microbe size and selectively release neutrophil extracellular traps in response to large pathogens. Nat Immunol 15:1017–1025. https://doi.org/10.1038/ni.2987.
44. Byrd MS, Pang B, Mishra M, Swords WE, Wozniak DJ. 2010. The Pseudomonas aeruginosa exopolysaccharide Psl facilitates surface adherence and NF-kappaB activation in A549 cells. mBio 1:e00140-10. https://doi.org/10.1128/mBio.00140-10.
45. Briheim G, Stendahl O, Dahlgren C. 1984. Intra- and extracellular events in luminol-dependent chemiluminescence of polymorphonuclear leukocytes. Infect Immun 45:1–5. https://doi.org/10.1128/IAI.45.1.1-5.1984.
46. Bjarnsholt T, Jensen PO, Burmolle M, Hentzer M, Haagensen JA, Hougen HP,

Calum H, Madsen KG, Moser C, Molin S, Hoiby N, Givskov M. 2005. Pseudomonas aeruginosa tolerance to tobramycin, hydrogen peroxide and polymorphonuclear leukocytes is quorum-sensing dependent. Microbiology (Reading) 151:373–383. https://doi.org/10.1099/mic.0.27463-0.
47. Lovewell RR, Patankar YR, Berwin B. 2014. Mechanisms of phagocytosis and host clearance of Pseudomonas aeruginosa. Am J Physiol Lung Cell Mol Physiol 306:L591–L603. https://doi.org/10.1152/ajplung.00335.2013.
48. Jensen ET, Kharazmi A, Garred P, Kronborg G, Fomsgaard A, Mollnes TE, Hoiby N. 1993. Complement activation by Pseudomonas aeruginosa biofilms. Microb Pathog 15:377–388. https://doi.org/10.1006/mpat.1993.1087.
49. Pamp SJ, Tolker-Nielsen T. 2007. Multiple roles of biosurfactants in structural biofilm development by Pseudomonas aeruginosa. J Bacteriol 189:2531–2539. https://doi.org/10.1128/JB.01515-06.
50. Rybtke M, Berthelsen J, Yang L, Hoiby N, Givskov M, Tolker-Nielsen T. 2015. The LapG protein plays a role in Pseudomonas aeruginosa biofilm formation by controlling the presence of the CdrA adhesin on the cell surface. Microbiologyopen 4:917–930. https://doi.org/10.1002/mbo3.301.
51. Bjarnsholt T, Jensen PO, Alhede M. 2019. Revival of Krebs-Ringer balanced salt solution for the investigation of polymorphonuclear leukocytes and Pseudomonas aeruginosa biofilm interaction. Pathog Dis 77:ftz052. https://doi.org/10.1093/femspd/ftz052.
52. Hmelo LR, Borlee BR, Almblad H, Love ME, Randall TE, Tseng BS, Lin C, Irie Y, Storek KM, Yang JJ, Siehnel RJ, Howell PL, Singh PK, Tolker-Nielsen T, Parsek MR, Schweizer HP, Harrison JJ. 2015. Precision-engineering the Pseudomonas aeruginosa genome with two-step allelic exchange. Nat Protoc 10:1820–1841. https://doi.org/10.1038/nprot.2015.115.
53. Koch B, Jensen LE, Nybroe O. 2001. A panel of Tn7-based vectors for insertion of the gfp marker gene or for delivery of cloned DNA into Gram-negative bacteria at a neutral chromosomal site. J Microbiol Methods 45:187–195. https://doi.org/10.1016/s0167-7012(01)00246-9.
54. Choi KH, Gaynor JB, White KG, Lopez C, Bosio CM, Karkhoff-Schweizer RR, Schweizer HP. 2005. A Tn7-based broad-range bacterial cloning and expression system. Nat Methods 2:443–448. https://doi.org/10.1038/nmeth765.
55. Choi KH, Kumar A, Schweizer HP. 2006. A 10-min method for preparation of highly electrocompetent Pseudomonas aeruginosa cells: application for DNA fragment transfer between chromosomes and plasmid transformation. J Microbiol Methods 64:391–397. https://doi.org/10.1016/j.mimet.2005.06.001.
56. Müsken M, Di Fiore S, Dotsch A, Fischer R, Haussler S. 2010. Genetic determinants of Pseudomonas aeruginosa biofilm establishment. Microbiology (Reading) 156:431–441. https://doi.org/10.1099/mic.0.033290-0.
57. Stover CK, Pham XQ, Erwin AL, Mizoguchi SD, Warrener P, Hickey MJ, Brinkman FS, Hufnagle WO, Kowalik DJ, Lagrou M, Garber RL, Goltry L, Tolentino E, Westbrock-Wadman S, Yuan Y, Brody LL, Coulter SN, Folger KR, Kas A, Larbig K, Lim R, Smith K, Spencer D, Wong GK, Wu Z, Paulsen IT, Reizer J, Saier MH, Hancock RE, Lory S, Olson MV. 2000. Complete genome sequence of Pseudomonas aeruginosa PAO1, an opportunistic pathogen. Nature 406:959–964. https://doi.org/10.1038/35023079.
58. Rybtke MT, Borlee BR, Murakami K, Irie Y, Hentzer M, Nielsen TE, Givskov M, Parsek MR, Tolker-Nielsen T. 2012. Fluorescence-based reporter for gauging cyclic di-GMP levels in Pseudomonas aeruginosa. Appl Environ Microbiol 78:5060–5069. https://doi.org/10.1128/AEM.00414-12.
59. Goltermann L, Tolker-Nielsen T. 2017. Importance of the exopolysaccharide matrix in antimicrobial tolerance of Pseudomonas aeruginosa aggregates. Antimicrob Agents Chemother 61:e02696-16. https://doi.org/10.1128/AAC.02696-16.
60. Kessler B, de Lorenzo V, Timmis KN. 1992. A general system to integrate lacZ fusions into the chromosomes of gram-negative eubacteria: regulation of the Pm promoter of the TOL plasmid studied with all controlling elements in monocopy. Mol Gen Genet 233:293–301. https://doi.org/10.1007/BF00587591.